Table 2 Tumor responses according to NLR

Response* to HAIC	All ($n = 266$)	High NLR ($n = 133$)	Low NLR ($n = 133$)
CR	16 (6.0)	3 (2.3)	13 (9.8)
PR	62 (23.3)	25 (18.8)	37 (27.8)
SD	83 (31.2)	40 (30.1)	43 (32.3)
PD	90 (33.8)	55 (41.4)	35 (26.3)
NE	15 (5.6)	10 (7.5)	5 (3.8)
Objective response rate	29.3%	21.1%	37.6%
		$P < 0.01$**	

*RECIST version 1.1, **χ^2-test.
Data are presented as n (%).
CR, complete response; HAIC, hepatic arterial infusion chemotherapy; NE, not evaluated; NLR, neutrophil to lymphocyte ratio; PD, progressive disease; PR, partial response; SD, stable disease.

Table 2. The objective response rate was 37.6% in patients with low NLR, which was significantly better than that of the patients with high NLR (21.1%; $P < 0.01$). Multivariate logistic regression analysis revealed that low NLR (hazard ratio [HR], 1.918; $P = 0.024$) as well as vascular invasion (HR, 1.874; $P = 0.029$) and extrahepatic lesion (HR, 2.723; $P = 0.012$) remained independently associated with the response to HAIC (Table 3).

The median PFS of all patients was 4.5 months. The PFS of patients with high NLR was shorter than that of the patients with low NLR, and the median PFS of the patients with high NLR was 3.2 months, which was significantly worse than that of the patients with low NLR of 5.6 months (Fig. 1a). The following nine of the

Table 3 Pretreatment factors affecting objective response

		n	ORR (%)	Univariate P*	Hazard ratio (95% CI)	Multivariate P**
NLR	<2.87	133	37.6	<0.01	1.918 (1.092–3.369)	0.024
	≥2.87	133	21.1			
Age, years	≥67	136	31.6	0.40		
	<67	130	26.9			
Sex	Male	209	29.7	0.81		
	Female	57	28.1			
ECOG PS	0	220	32.3	0.051		
	1	41	17.1			
	2	5	0			
Prior treatment of sorafenib	Absence	241	29.5	0.88		
	Presence	25	28.0			
HBs antigen	Positive	70	32.9	0.45		
	Negative	196	28.1			
HCV antibody	Positive	146	31.5	0.39		
	Negative	120	26.7			
Child–Pugh score	5–6	134	35.8	0.054		
	7	55	25.5			
	8–9	77	20.8			
Vascular invasion	Absence	137	36.5	<0.01	1.874 (1.067–3.292)	0.029
	Presence	129	21.7			
Extrahepatic lesion	Absence	205	33.7	<0.01	2.723 (1.250–5.932)	0.012
	Presence	61	14.8			
CRP, mg/dL	<0.8	127	33.9	0.11		
	≥0.8	136	25.0			
AFP, ng/mL	<235.5	133	31.6	0.42		
	≥235.5	133	27.1			
DCP, mAU/mL	<567	133	33.8	0.11		
	≥567	133	24.8			

*χ^2-Test, **logistic regression analysis.
AFP, α-fetoprotein; CI, confidence interval; CRP, C-reactive protein; DCP, des-γ-carboxyprothrombin; ECOG PS, Eastern Cooperative Oncology Group performance status; HBs antigen, hepatitis B surface antigen; HCV antibody, hepatitis C virus antibody; NLR, neutrophil to lymphocyte ratio; ORR, objective response rate.
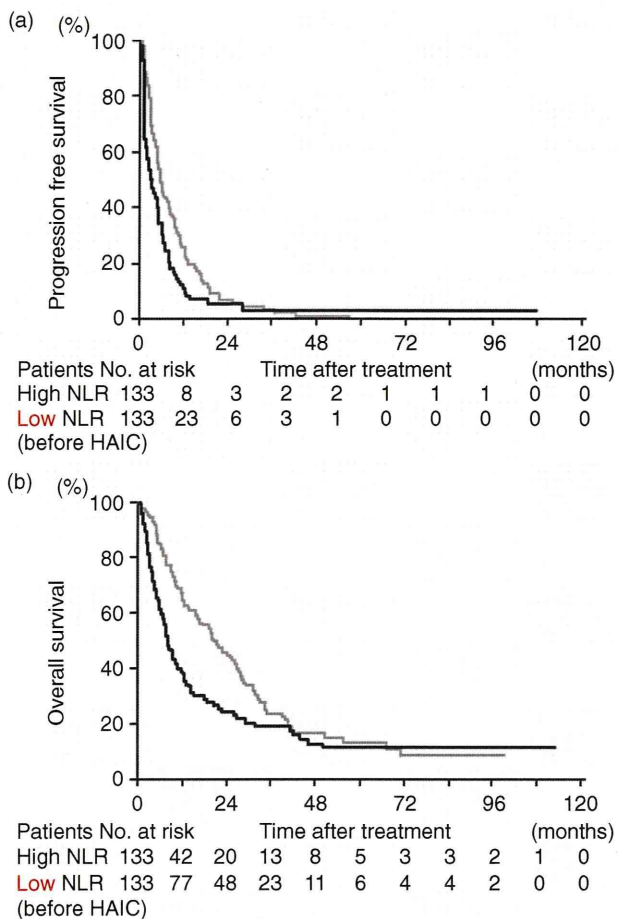
Figure 1 Kaplan–Meier plot of progression-free survival (PFS) and overall survival (OS) since commencement of HAIC according to neutrophil to lymphocyte ratio (NLR). (a) Median PFS of the patients with high NLR was 3.2 months, which was significantly worse than that of the patients with low NLR, 5.6 months ($P < 0.01$). (b) Median OS of the patients with high NLR was 8.0 months, which was significantly worse than that of the patients with low NLR, 20.7 months ($P < 0.01$). ——, High NLR; ——, Low NLR.

12 pretreatment variables were significantly associated with the PFS times in univariate analyses: ECOG PS ($P < 0.01$), hepatitis B surface antigen (HBsAg; $P < 0.01$), hepatitis C virus antibody ($P = 0.044$), vascular invasion ($P < 0.01$), extrahepatic lesion ($P < 0.01$), CRP ($P < 0.01$), α-fetoprotein (AFP) ($P < 0.01$) and DCP ($P < 0.01$) as well as NLR. Pretreatment high NLR was an independent unfavorable factor for PFS (HR, 1.363; $P = 0.044$) as well as ECOG PS 1 and 2 (HR compared with ECOG PS, 1.585; $P = 0.019$ and 3.301; $P = 0.025$, respectively), HBsAg positive (HR, 1.687; $P < 0.01$),

extrahepatic lesion (HR, 1.500; $P = 0.025$) and AFP of 235.5 ng/mL or more (HR, 1.580; $P < 0.01$) in Cox's proportional hazards regression model (Table 4).

Patient outcome stratified by pretreatment NLR

The median OS of all patients was 12.6 months. The OS in the patients with high NLR was shorter than that of the patients with low NLR ($P < 0.01$), and the median OS in the patients with high NLR was 8.0 months, which was significantly worse than that of the patients with low NLR (20.7 months) (Fig. 1b). The following eight of the 12 pretreatment variables were significantly associated with the OS in univariate analyses: ECOG PS ($P < 0.01$), Child–Pugh score ($P < 0.01$), vascular invasion ($P < 0.01$), extrahepatic lesion ($P < 0.01$), CRP ($P < 0.01$), AFP ($P < 0.01$) and DCP ($P < 0.01$) as well as NLR. Pretreatment high NLR was an independent unfavorable factor for OS (HR, 1.492; $P < 0.01$) as well as ECOG PS 1 and 2 (HR compared with ECOG PS 0, 1.597; $P = 0.034$ and 3.825; $P = 0.013$, respectively), Child–Pugh score 8 or 9 (HR compared with Child–Pugh score 5 or 6, 1.454; $P = 0.036$), extrahepatic lesion (HR, 1.677; $P < 0.01$), CRP of 0.8 or more (HR, 1.406; $P = 0.031$) and AFP of 235.5 or more (HR, 1.702; $P < 0.01$) in Cox's proportional hazards regression model (Table 5).

Patient outcome according to trend of NLR

We obtained the NLR value at 4 weeks after the start of HAIC in 243 patients. Of the patients with high NLR before HAIC ($n = 120$), NLR was low at 4 weeks after the start of HAIC (High-Low) in 69 patients (57.5%). The median PFS in the patients with High-Low was 4.9 months, which was significantly better than that of the patients with high NLR at 4 weeks after the start of HAIC (High-High), 2.0 months ($P = 0.030$). The median OS in the patients with High-Low was 11.5 months, which was significantly better than that of the patients with High-High, 6.1 months ($P < 0.01$) (Fig. 2a). In contrast, of the patients with low NLR before HAIC ($n = 123$), NLR was high at 4 weeks after the start of HAIC (Low-High) in 11 (8.9%) patients. The median PFS in the patients with Low-High was 2.0 months, which was significantly worse than that of the patients with low NLR at 4 weeks after the start of HAIC (Low-Low), 6.0 months ($P < 0.01$). The median OS in the patients with Low-High was 5.5 months, which was significantly worse than that of the patients with Low-Low, 22.6 months ($P < 0.01$) (Fig. 2b).

Table 4 Pretreatment factors affecting progression-free survival

		n	mPFS (months)	Univariate P*	Hazard ratio (95% CI)	Multivariate P**
NLR	≥2.87	133	3.2	<0.01	1.363 (1.008–1.843)	0.044
	<2.87	133	5.6			
Age, years	<67	130	4.0	0.46		
	≥67	136	5.2			
Sex	Male	209	4.5	0.31		
	Female	57	5.1			
ECOG PS	2	5	0.9	<0.01	3.301 (1.165–9.355)	0.025
	1	41	2.7		1.585 (1.079–2.330)	0.019
	0	220	4.9			
Prior treatment of sorafenib	Absence	241	4.5	0.95		
	Presence	25	4.8			
HBs antigen	Positive	70	2.5	<0.01	1.687 (1.163–2.447)	<0.01
	Negative	196	5.5			
HCV antibody	Negative	120	3.1	0.044	0.841 (0.596–1.188)	0.33
	Positive	146	5.5			
Child–Pugh score	8–9	77	3.2	0.099		
	7	55	4.5			
	5–6	134	5.1			
Vascular invasion	Presence	129	2.7	<0.01	1.191 (0.876–1.619)	0.27
	Absence	137	6.2			
Extrahepatic lesion	Presence	61	2.8	<0.01	1.500 (1.053–2.138)	0.025
	Absence	205	5.5			
CRP, mg/dL	≥0.8	136	2.8	<0.01	1.293 (0.952–1.758)	0.10
	<0.8	127	6.2			
AFP, ng/mL	≥235.5	133	2.8	<0.01	1.580 (1.162–2.148)	<0.01
	<235.5	133	6.2			
DCP, mAU/mL	≥567	133	3.2	<0.01	1.203 (0.873–1.659)	0.26
	<567	133	5.6			

*Log–rank test, **Cox's proportional hazards regression model.
AFP, α-fetoprotein; CI, confidence interval; CRP, C-reactive protein; DCP, des-γ-carboxyprothrombin; ECOG PS, Eastern Cooperative Oncology Group performance status; HBs antigen, hepatitis B surface antigen; HCV antibody, hepatitis C virus antibody; mPFS, median progression-free survival time; NLR, neutrophil to lymphocyte ratio.

Correlation between cytokine or chemokine profiling and NLR

Data of cytokine and chemokine profiling were obtained in 86 patients. We investigated the association between the value of cytokine or chemokine and NLR to analyze the mechanisms of NLR to cancer biology. Results are shown in Table 6. Serum PDGF-BB concentration had a significant positive correlation with NLR ($r = 0.227$; $P = 0.035$) (Fig. S1). No other cytokine or chemokine was correlated with NLR.

DISCUSSION

THE FIRST AIM of this study was to investigate the correlation between NLR and patient characteristics in advanced HCC. Some reports have suggested that NLR is correlated with tumor biology in unselected cohorts of patients with HCC.[21] Our analysis also demonstrated the corresponding results in patients with HCC at an advanced stage. Moreover, it was newly clarified that NLR had a strong relation with ECOG PS, which was an important factor reflecting a variety of complications of liver cirrhosis or tumor-related symptoms.[22]

The most important insight of our study was that NLR was correlated with the treatment efficacies presented as response to HAIC or PFS as well as patient outcome given that this is the largest cohort of patients with advanced HCC treated with HAIC, to the best of our knowledge. Our results should be interpreted with caution because of the bias introduced by the differences of patient characteristics observed between the

Table 5 Pretreatment factors affecting overall survival

		n	mOS (months)	Univariate P*	Hazard ratio (95% CI)	Multivariate P**
NLR	≥2.87	133	8.0	<0.01	1.492 (1.106–2.012)	<0.01
	<2.87	133	20.7			
Age, years	<67	130	9.9	0.18		
	≥67	136	17.7			
Sex	Female	57	10.7	0.091		
	Male	209	13.6			
ECOG PS	2	5	2.4	<0.01	3.825 (1.329–11.009)	0.013
	1	41	7.3		1.597 (1.035–2.463)	0.034
	0	220	14.5			
Prior treatment of sorafenib	Presence	25	11.6	0.77		
	Absence	241	13.1			
HBs antigen	Positive	70	8.4	0.095		
	Negative	196	15.4			
HCV antibody	Negative	120	10.7	0.096		
	Positive	146	16.6			
Child–Pugh score	8–9	77	6.9	<0.01	1.454 (1.024–2.064)	0.036
	7	55	13.7		0.942 (0.621–1.429)	0.78
	5–6	134	16.6			
Vascular invasion	Presence	129	8.2	<0.01	1.138 (0.819–1.582)	0.44
	Absence	137	19.6			
Extrahepatic lesion	Presence	61	6.5	<0.01	1.677 (1.144–2.458)	<0.01
	Absence	205	16.6			
CRP, mg/dL	≥0.8	136	8.7	<0.01	1.406 (1.031–1.917)	0.031
	<0.8	127	22.6			
AFP, ng/mL	≥235.5	133	8.7	<0.01	1.702 (1.228–2.359)	<0.01
	<235.5	133	21.8			
DCP, mAU/mL	≥567	133	9.0	<0.01	1.123 (0.808–1.568)	0.49
	<567	133	20.7			

*Log–rank test, **Cox's proportional hazards regression model.
AFP, α-fetoprotein; CI, confidence interval; CRP, C-reactive protein; DCP, des-γ-carboxyprothrombin; ECOG PS, Eastern Cooperative Oncology Group performance status; HBs antigen, hepatitis B surface antigen; HCV antibody, hepatitis C virus antibody; mOS, median overall survival time; NLR, neutrophil to lymphocyte ratio.

high NLR group and low NLR group. However, our results suggested that NLR was a predictor of response to HAIC in multivariate analysis independent of ECOG PS, hepatic reserve and tumor-related factors in this study. CRP was suggested as a prognostic marker for patients with HCC treated with sorafenib;[23] however, it remains unclear whether such factors can predict antitumor effects of sorafenib or the prognosis of patients with advanced HCC. NLR may be a stronger predictor than CRP of both of antitumor effects and prognosis of patients with advanced HCC treated with HAIC. The differential leukocyte count is an inexpensive and routinely measured marker in daily clinical practice and, therefore, NLR is a simple and easily available marker for the selection of suitable patients to undergo HAIC.

Another interesting point of the present study was that the cumulative survival curve was stratified according to trend of NLR before and after HAIC. The antitumor effect was evaluated generally by radiological findings and the trends of tumor markers, such as AFP or DCP in HCC.[24] However, these modalities have disadvantages such as complications, cost of measurements and lack of universality because the evaluation was often difficult to interpret.[25] Further, tumor markers were not elevated in one-third of the patients with HCC.[17] Our findings suggested that NLR, a simple and economical marker derived from routinely available blood tests, was helpful in evaluating the efficacy of HAIC or predicting the outcomes of the patients with advanced HCC by following its trend.
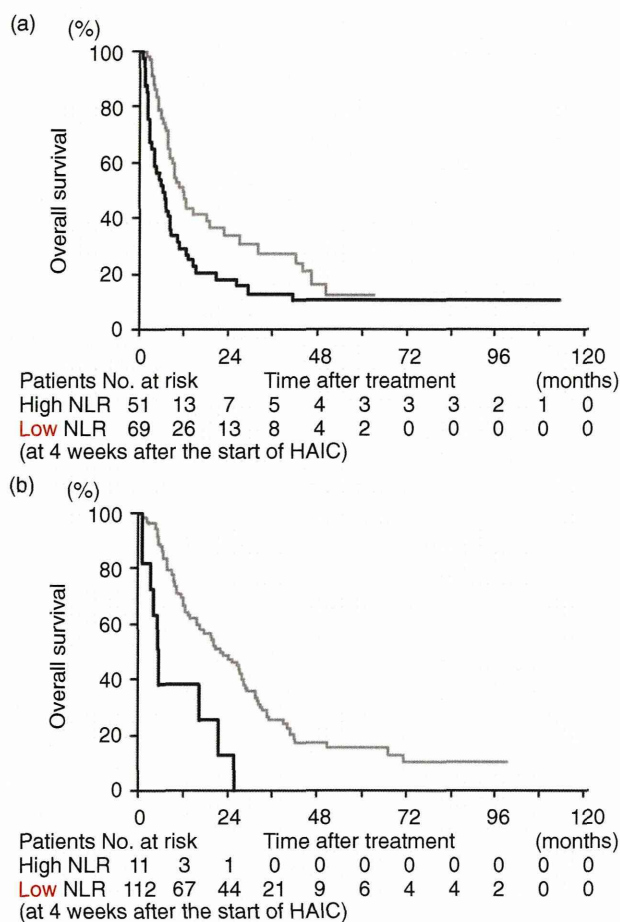
(a)

(b)

Figure 2 Kaplan–Meier plot of overall survival (OS) since commencement of hepatic arterial infusion chemotherapy (HAIC) according to neutrophil to lymphocyte ratio (NLR) at 4 weeks after the start of treatment. (a) Among the patients with high NLR before HAIC, median OS of the patients whose NLR was reduced (High-Low) was 11.5 months, which was significantly better than that of the patients with remaining high NLR (High-High), 6.1 months ($P < 0.01$). (b) Among the patients with low NLR before HAIC, median OS of the patients whose NLR was elevated (Low-High) was 5.5 months, which was significantly worse than that of the patients with remaining low NLR (Low-Low), 22.6 months ($P < 0.01$).

Finally, our findings indicated that PDGF-BB was a candidate of mediators for NLR, reflecting tumor biology and response to HAIC. It was reported that activated neutrophils stimulate the growth and progression of the cancer cells by releasing growth factors such as PDGF-BB.[26] It has been shown that PDGF-BB also promotes angiogenesis and subsequent vascular invasion[27] and may reduce the sensitivity to cytotoxic agents in HCC.[28] Some reports stated that the serum level of PDGF-BB correlated with the efficacy of treatments for HCC,[27,29] and should be paid more attention when considering treatment of patients with HCC.

The present study has several limitations. For instance, the study was retrospective in nature and it was conducted at a single center. Therefore, further study is needed to validate our findings.

In conclusion, high NLR was strongly correlated with poor general condition and advanced tumor progression in patients with advanced HCC. NLR can act as a predictive and prognostic factor for patients with advanced HCC treated with HAIC. The trends of NLR after treatment of HAIC strongly reflected the patient outcomes in this study. Our findings can be useful in determining treatment strategies or in designing future clinical chemotherapy trials of advanced HCC.

ACKNOWLEDGMENTS

Table 6 Association between cytokine or chemokine and NLR

	r	*P**
EGF	0.001	0.99
FGF	0.141	0.20
HGF	0.011	0.92
IFN-γ	0.132	0.23
IL-2	0.103	0.35
IL-4	0.161	0.14
TNF-α	0.124	0.26
IL-6	0.159	0.15
IL-8	−0.080	0.47
IL-10	0.121	0.27
IL-5	−0.035	0.75
IP10	−0.089	0.42
MIG	−0.112	0.31
PDGF-BB	0.227	0.035
TGF-β	0.000	1.00
TGF-α	−0.041	0.71
VEGF	−0.102	0.35
SCF	−0.088	0.42
IL-12	0.040	0.71
SDF-1	−0.077	0.48

*Linear regression.
EGF, epidermal growth factor; FGF, fibroblast growth factor; HGF, hepatocyte growth factor; IFN, interferon; IL, interleukin; IP, interferon-γ-induced protein, MIG, monokine induced by interferon-γ; PDGF, platelet-derived growth factor; SCF, stem cell factor; SDF, stromal cell-derived factor; TGF, transforming growth factor; TNF, tumor necrosis factor; VEGF, vascular endothelial growth factor.

REFERENCES

1 Ferlay J, Shin HR, Bray F, Forman D, Mathers C, Parkin DM. Estimates of worldwide burden of cancer in 2008: GLOBOCAN 2008. *Int J Cancer* 2010; 127: 2893–917.

2 Lee JM, Yoon JH, Kim KW. Diagnosis of hepatocellular carcinoma: newer radiological tools. *Semin Oncol* 2012; 39: 399–409.

3 Takizawa D, Kakizaki S, Sohara N *et al.* Hepatocellular carcinoma with portal vein tumor thrombosis: clinical characteristics, prognosis, and patient survival analysis. *Dig Dis Sci* 2007; 52: 3290–5.

4 Llovet JM, Ricci S, Mazzaferro V *et al.* Sorafenib in advanced hepatocellular carcinoma. *N Engl J Med* 2008; 359: 378–90.

5 Kaneko S, Furuse J, Kudo M *et al.* Guideline on the use of new anticancer drugs for the treatment of Hepatocellular Carcioma 2010 update. *Hepatol Res* 2012; 42: 523–42.

6 Terashima T, Yamashita T, Arai K *et al.* Feasibility and efficacy of hepatic arterial infusion chemotherapy for advanced hepatocellular carcinoma after sorafenib. *Hepatol Research* 2014; 44: 1179–85.

7 Song DS, Song MJ, Bae SH *et al.* A comparative study between sorafenib and hepatic arterial infusion chemotherapy for advanced hepatocellular carcinoma with portal vein tumor thrombosis. *J Gastroenterol* 2014; [Epub ahead of print]. doi: 10.1007/s00535-014-0978-3.

8 Mantovani A, Allavena P, Sica A, Balkwill F. Cancer-related inflammation. *Nature* 2008; 454: 436–44.

9 Grivennikov SI, Greten FR, Karin M. Immunity, inflammation, and cancer. *Cell* 2010; 140: 883–99.

10 Chen L, Zhang Q, Chang W, Du Y, Zhang H, Gao G. Viral and host inflammation-related factors that can predict the prognosis of hepatocellular carcinoma. *Eur J Cancer* 2012; 48: 1977–87.

11 Templeton AJ, McNamara MG, Seruga B *et al.* Prognostic role of neutrophil-to-lymphocyte ratio in solid tumors: a systematic review and meta-analysis. *J Natl Cancer Inst* 2014; [Epub ahead of print]. doi: 10.1093/jnci/dju124.

12 Bertuzzo VR, Cescon M, Ravaioli M *et al.* Analysis of factors affecting recurrence of hepatocellular carcinoma after liver transplantation with a special focus on inflammation markers. *Transplantation.* 2011; 91: 1279–85.

13 Chen TM, Lin CC, Huang PT, Wen CF. Neutrophil-to-lymphocyte ration associated with mortality in early hepatocellular carcinoma patients after radiofrequency ablation. *J Gastroenterol Hepatol* 2012; 27: 553–61.

14 McNally ME, Martinez A, Khabiri H *et al.* Inflammatory markers are associated with outcome in patients with unresectable hepatocellular carcinoma undergoing transarterial chemoembolization. *Ann Surg Oncol* 2013; 20: 923–8.

15 Motomura T, Shirabe K, Mano Y *et al.* neutrophil-lymphocyte ratio reflects hepatocellular carcinoma recurrence after liver transplantation via inflammatory microenvironment. *J Hepatol* 2013; 58: 58–64.

16 Pinato DJ, Sharma R. An inflammation-based prognostic index predicts survival advantage after transarterial chemoembolization in hepatocellular carcinoma. *Transl Res* 2012; 160: 146–52.

17 Bruix J, Sherman M, Practice Guidelines Committee, American Association for the Study of Liver Diseases. Management of hepatocellular carcinoma. *Hepatology* 2005; 42: 1208–36.

18 Yamashita T, Arai K, Sunagozaka H *et al.* Randomized, phase II study comparing interferon combined with hepatic arterial infusion of fluorouracil plus cisplatin and fluorouracil alone in patients with advanced hepatocellular carcinoma. *Oncology* 2011; 81: 281–90.

19 Arihara F, Mizukoshi E, Kitahara M *et al.* Increase of CD14+HLA-DR-/low myeloid-derived suppressor cells in hepatocellular carcinoma patients and its impact on prognosis. *Cancer Immunol Immunother* 2013; 62: 1421–30.

20 Eisenhauer EA, Therasse P, Bogaerts J *et al.* New response evaluation criteria in solid tumours: revised RECIST guideline (version 1.1). *Eur J Cancer* 2009; 45: 228–47.

21 Pinato DJ, Stebbing J, Ishizuka M *et al.* A novel and validated prognostic index in hepatocellular carcinoma: the inflammation based index (IBI). *J Hepatol* 2012; 57: 1013–20.

22 Hsu CY, Lee YH, Hsia CY *et al.* Performance status in patients with hepatocellular carcinoma: determinants, prognostic impact, and ability to improve the Barcelona Clinic Liver Cancer System. *Hepatology* 2013; 57: 112–19.

23 Morimoto M, Numata K, Moriya S *et al.* Inflammation-based prognostic score for hepatocellular carcinoma patients on sorafenib treatment. *Anticancer Res* 2012; 32: 619–23.

24 Lee MH, Kim SU, Kim do Y *et al.* Early on-treatment predictions of clinical outcome using alpha-fetoprotein and des-gamma-carboxy prothrombin responses in patients with advanced hepatocellular carcinoma. *J Gastroenterol Hepatol* 2012; 27: 313–22.

25 Oxnard GR, Morris MJ, Hodi FS *et al.* When progressive disease does not mean treatment failure: reconsidering the criteria for progression. *J Natl Cancer Inst* 2012; 104: 1534–41.

26 Wada Y, Yoshida K, Tsutani Y *et al.* Neutrophil elastase induces cell proliferation and migration by the release of TGF-alpha, PDGF and VEGF in esophageal cell lines. *Oncol Rep* 2007; 17: 161–7.

27 Miyahara K, Nouso K, Morimoto Y *et al.* Pro-angiogenic cytokines for prediction of outcomes in patients with advanced hepatocellular carcinoma. *Br J Cancer* 2013; 109: 2072–8.

28 Lau CK, Yang ZF, Ho DW *et al.* An Akt/Hypoxia-inducible factor-1alpha/platelet-derived growth factor-BB autocrine loop mediates hypoxia-induced chemoresistance in liver
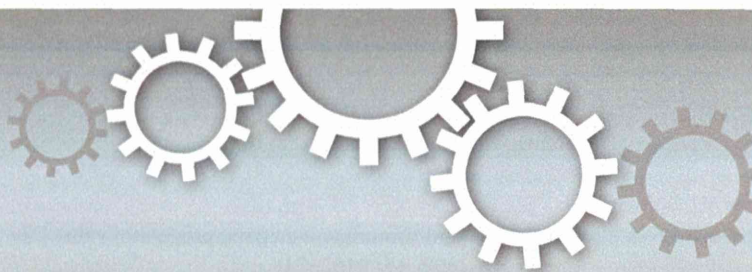
cancer cells and tumorigenic hepatic progenitor cells. *Clin Cancer Res* 2009; **15**: 3462–71.

29 Inaba Y, Kanai F, Aramaki T *et al.* A randomized phase II study of TSU-68 in patients with hepatocellular carcinoma treated by transarterial chemoembolization. *Eur J Cancer* 2013; **49**: 2832–40.

SUPPORTING INFORMATION

A DDITIONAL SUPPORTING INFORMATION may be found in the online version of this article at the publisher's website:

Figure S1 Relationship between overall survival and platelet-derived growth factor (PDGF)-BB. PDGF-BB concentration had significant positive correlation with neutrophil to lymphocyte ratio (NLR) on the basis of weighted linear regression (r = 0.227; *P* = 0.035).

SCIENTIFIC REPORTS

Small tRNA-derived RNAs are increased and more abundant than microRNAs in chronic hepatitis B and C

Sara R. Selitsky[1,2,3,4], Jeanette Baran-Gale[1,2], Masao Honda[5], Daisuke Yamane[3,4], Takahiro Masaki[3,4], Emily E. Fannin[2], Bernadette Guerra[6], Takayoshi Shirasaki[5], Tetsuro Shimakami[5], Shuichi Kaneko[5], Robert E. Lanford[6], Stanley M. Lemon[3,4]* & Praveen Sethupathy[1,2,4]*

[1]Bioinformatics and Computational Biology Curriculum, University of North Carolina at Chapel Hill, Chapel Hill, North Carolina, United States of America, [2]Department of Genetics, University of North Carolina at Chapel Hill, Chapel Hill, North Carolina, United States of America, [3]Departments of Medicine and Microbiology & Immunology, University of North Carolina at Chapel Hill, Chapel Hill, North Carolina, United States of America, [4]Lineberger Comprehensive Cancer Center, University of North Carolina at Chapel Hill, Chapel Hill, North Carolina, United States of America, [5]Department of Gastroenterology, Kanazawa University Graduate School of Medicine, Kanazawa, Japan, [6]Department of Virology and Immunology, Texas Biomedical Research Institute and Southwest National Primate Research Center, San Antonio, Texas, United States of America.

Persistent infections with hepatitis B virus (HBV) or hepatitis C virus (HCV) account for the majority of cases of hepatic cirrhosis and hepatocellular carcinoma (HCC) worldwide. Small, non-coding RNAs play important roles in virus-host interactions. We used high throughput sequencing to conduct an unbiased profiling of small (14–40 nts) RNAs in liver from Japanese subjects with advanced hepatitis B or C and hepatocellular carcinoma (HCC). Small RNAs derived from tRNAs, specifically 30–35 nucleotide-long 5′ tRNA-halves (5′ tRHs), were abundant in non-malignant liver and significantly increased in humans and chimpanzees with chronic viral hepatitis. 5′ tRH abundance exceeded microRNA abundance in most infected non-cancerous tissues. In contrast, in matched cancer tissue, 5′ tRH abundance was reduced, and relative abundance of individual 5′ tRHs was altered. In hepatitis B-associated HCC, 5′ tRH abundance correlated with expression of the tRNA-cleaving ribonuclease, angiogenin. These results demonstrate that tRHs are the most abundant small RNAs in chronically infected liver and that their abundance is altered in liver cancer.

epatitis B virus (HBV) and hepatitis C virus (HCV) are phylogenetically unrelated non-cytopathic viruses that infect the liver[1]. While HBV is a DNA virus, and HCV is a positive-strand RNA virus, both have the capacity to persist for years in some infected individuals. Hundreds of millions of people worldwide are chronic carriers of HBV or HCV, 30–50% of whom have chronic liver disease[2]. Together, these viral infections are responsible for ~60% of liver cirrhosis and ~80% of hepatocellular carcinoma (HCC), a leading cause of cancer-related deaths worldwide. Numerous studies suggest that microRNAs (miRNAs), small 21–23 nt non-coding RNAs are important in the pathogenesis of these infections, modulating viral replication as well as host responses and possibly influencing the risk of carcinogenesis[3]. For example the HBV X protein represses expression of miR-148a, potentially enhancing tumorigenesis[4]. In contrast, HCV infection is associated with higher expression of miR-21, which targets key components of Toll-like receptor signaling pathways, possibly facilitating viral evasion of innate immune responses[5]. miR-122 stabilizes HCV RNA and promotes its replication[6,7], and the importance of this interaction is reflected in the clinical development of an anti-miR-122 antagomir (miravirsen) as an antiviral therapeutic[8].

Somewhat larger, 30–35 nt RNAs derived from the 5′ half of tRNA (5′ tRHs) represent a second major class of small non-coding RNA[9]. Increased expression of 5′ tRHs has been associated with viral and rickettsial infections in animals[10,11], and may serve to prevent apoptosis and promote cell survival[12]. However, they have not been studied previously in the context of viral hepatitis. To our knowledge, only one study has described unbiased profiling of small RNAs in the liver during chronic viral hepatitis[13], but the analysis was restricted to miRNAs. We sequenced small (14–40 nts) RNAs in liver biopsies from subjects with chronic hepatitis and HCC, examining both non-tumor and matched cancer tissue, and found a surprisingly high proportion of reads representing 5′ tRHs[9]. Our results document their presence in human tissue, demonstrate that they are the most highly abundant
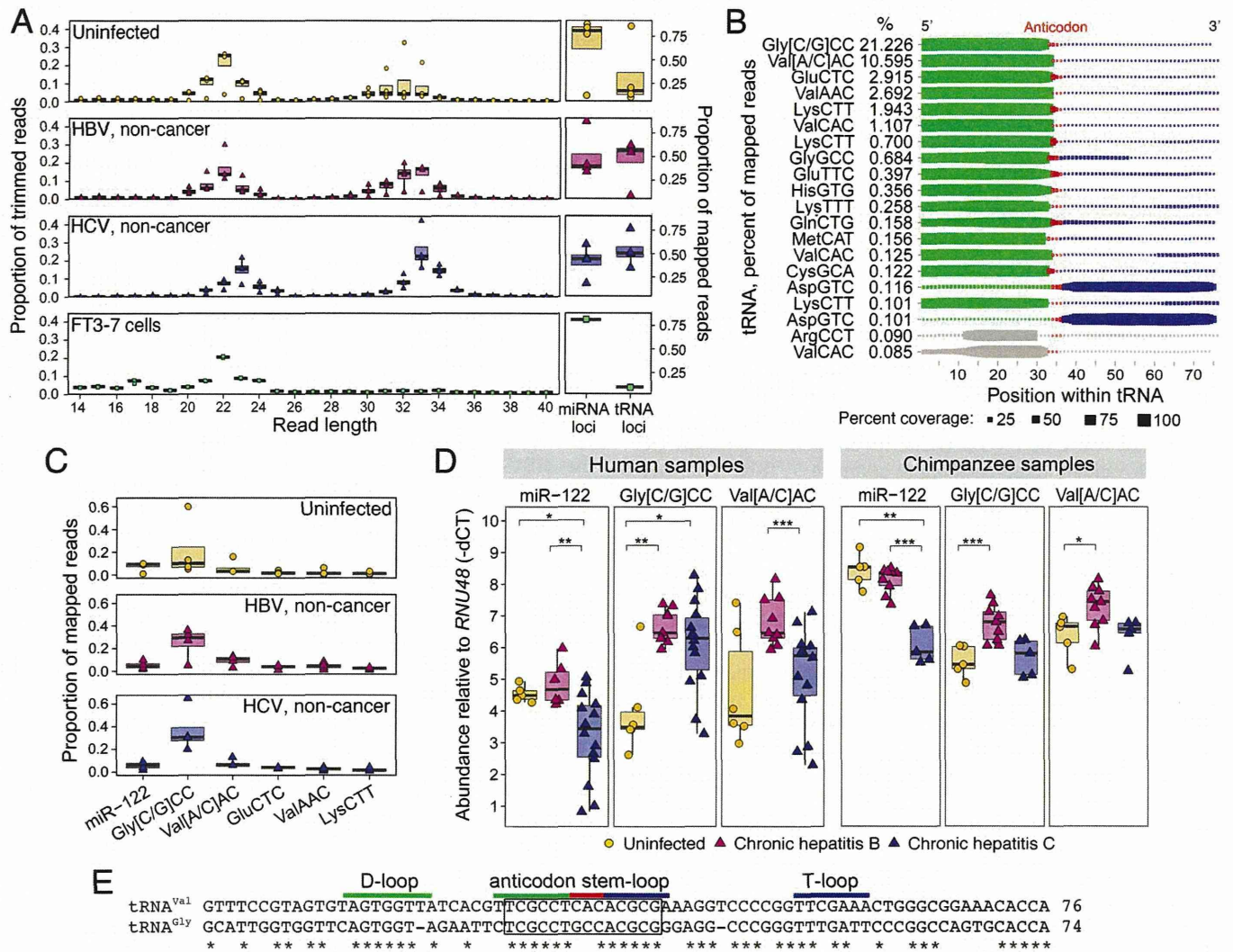
Figure 1 | tRH abundance in HBV- and HCV-infected liver. (a) (left) Read length distribution of 14–40 nt RNAs in non-malignant liver from uninfected, HBV-, or HCV-infected subjects ($n=4$ each), and FT3-7 cells ($n=3$ replicates). (right) Proportion of reads mapping to miRNA versus tRNA loci. Boxes represent median ± 1.5 * interquartile range. (b) tRNA coverage plot from the average of the 20 non-cancer samples. Dot size represents percent of reads mapping at each base position within each tRNA (top 20 by average abundance). The anticodon is red, with 5′ bases green and 3′ bases blue. Gray: bases of RNAs that are non-tRHs. See Supplemental Figure 1. (c) Proportion of mapped reads aligning to miR-122 versus the five most abundant tRNA-derived RNAs. (d) (left) Expression levels (RT-qPCR) of miR-122, 5′ tRH[Gly] ("Gly[C/G]CC") and 5′ tRH[Val] ("Val[A/C]AC") in uninfected ($n=5$–6), HBV-infected ($n=6$–9) and HCV-infected ($n=14$) human liver. Numbers of samples differ due to limited RNA. (right) Similar results from uninfected ($n=5$), HBV-infected ($n=9$), and HCV-infected C ($n=5$) chimpanzees. *RNU48* was used as a normalizer. *$P < 0.05$; **$P < 0.01$; ***$P < 0.005$ by Mann-Whitney U-test. (e) ClustalW[43] multiple sequence alignment of representative tRNA[Gly] and tRNA[Val] genes from which 5′ tRH[Gly] and 5′ tRH[Val] could originate (see Supplemental Figure 3). tRNAs regions are highlighted according to the color scheme in panel (b). The box identifies a unique conserved sequence motif described in the text. "Mapped reads" represents all reads aligning to miRNAs or tRNAs (see Methods).

small RNAs in virus-infected liver, and show that their abundance is altered in various disease states including hepatocellular carcinoma.

Results

tRNA-half abundance is significantly increased in chronic viral hepatitis.

We employed high-throughput sequencing to characterize the small RNA transcriptome in liver tissue from Japanese adults with advanced hepatitis B or hepatitis C and concomitant HCC (see Supplemental Table 1 for patient information; see Supplemental Tables 2–4 for summary statistics on RNA, qRT-PCR, and sequencing). Initial studies focused on non-malignant tissue from 4 subjects with hepatitis B (mean age 53 ± 4 yrs s.e.m.), 4 with hepatitis C (63 ± 2 yrs), and 4 uninfected individuals undergoing resection of metastatic tumors (60 ± 10 yrs)[14]. A large proportion of the sequencing reads were 19–25 nts in length (median 38%, range 10–73%), as expected for miRNAs[15] (Figure 1a, left). However, we

detected an equal or greater abundance of 30–35 nt reads in HBV- and HCV-infected liver (median 54%, range 14–80%). These larger RNAs were less abundant in uninfected tissue (median 21%, range 14–84%) and in human hepatoma (FT3-7) cells (median 9%, range 8.7–9.3%).

Most (~65%) of the 30–35 nt reads in infected samples aligned perfectly to the region 5′ of the anticodon triplet in annotated tRNA genes[16] (Figure 1b, Supplemental Figure 1, Supplemental Table 5 and 6). We refer to these as "5′ tRNA-halves" (5′ tRHs)[9]. Many of the remaining 30–35 nt reads also aligned to the 5′ end of tRNAs, particularly tRNA[Gly], but with one or more nucleotide deletions. Also present were 3′ tRHs (~36–39 nts) mapping to the region 3′ of the anticodon, including the 3′ terminal CCA (Figure 1b, Supplemental Figure 1). Additionally, we identified shorter reads derived from 3′ or 5′ tRNA termini, referred to previously as "tRNA fragments"[9] (tRFs), or the region immediately 5′ or 3′ of the anticodon loop, but these

were much less frequent. In 6 of 8 infected livers, more reads mapped to tRNA loci[16] than to known miRNAs[17] (see Methods), while the opposite was true in 3 of 4 uninfected tissues as well as FT3-7 cells (Figure 1a, right).

There are 625 annotated tRNA genes in the human genome (hg19) encoding 458 unique tRNA sequences. We identified reads mapping to 348 of these 458 sequences. Notably, in 11 of the 12 subjects, the same five 5′ tRHs comprised >80% of tRNA-derived reads (Supplemental Figure 2a). The two most abundant 5′ tRHs were Gly[C/G]CC ("5′ tRH^{Gly}"), which could be derived from any of 10 tRNA^{Gly} genes with identical 5′ sequence, and Val[A/C]AC ("5′ tRH^{Val}"), which could originate from any of 15 tRNA^{Val} genes (Figure 1b and C, Supplemental Figure 1 and 3, and Supplemental Table 5)[16]. 5′ tRH^{Gly} accounted for 54 ± 9% (s.d.) and 5′ tRH^{Val} 17 ± 9% of all tRNA-derived RNA reads (Supplemental Figure 2a). Remarkably, 5′ tRH^{Gly} abundance exceeded that of miR-122, one of the most abundant liver miRNAs[13], in 7 of 8 virus-infected tissues.

We used real-time reverse transcription quantitative PCR (RT-qPCR) to validate these results and compare 5′ tRH^{Gly}, 5′ tRH^{Val} and miR-122 abundance in liver tissue from 22 additional subjects (Supplemental Table 1–3)[14]. These analyses confirmed that 5′ tRH^{Gly} abundance was increased in HBV- and HCV-infected liver compared with uninfected tissues (P<0.01 and P<0.05, respectively) (Figure 1d, left). A similar trend was observed for 5′ tRH^{Val} (HBV P=0.07; HCV P=0.7). 5′ tRH^{Gly} and 5′ tRH^{Val} were more abundant than miR-122 in HBV- and HCV-infected liver (5′ tRH^{Gly}, P<0.005 for both HBV and HCV; 5′ tRH^{Val}, P<0.005 for HBV and P<0.01 for HCV) (Figure 1d left). Notably, 5′ tRH^{Val} abundance was higher in HBV- than in HCV-infected tissues (P<0.005).

Chimpanzees (Pan troglodytes) recapitulate many aspects of HBV and HCV infections in humans[18,19], and are free of potential confounding variables (e.g., alcohol intake, smoking) that are difficult to control in human cohorts. Similar to humans, we found that intrahepatic 5′ tRH^{Gly} and 5′ tRH^{Val} abundance was increased in archived liver tissue from chimpanzees chronically infected with HBV compared to uninfected animals (P<0.005 and P<0.05, respectively) (Figure 1d, right, and Supplemental Table 7). However, 5′ tRH abundance was not increased in chronically HCV-infected chimpanzee liver.

In human tissues, the relative abundance of specific tRNA-derived RNAs correlated with codon usage (codon frequency in DNA sequence) (Spearman's rho=0.32, P=0.01) and the number of possible tRNA genes from which each could originate (rho=0.41, P=0.001) (Supplemental Figure 2b). However, tRNAs representing potential sources of the five most abundant tRHs were not the most highly ranked by gene number or codon usage, suggesting that additional factors likely determine tRH biogenesis (Supplemental Figure 4). Interestingly, those tRNAs from which 5′ tRH^{Gly} and 5′ tRH^{Val} are potentially derived share a unique sequence motif in the anticodon stem-loop region (Figure 1e) not present in other tRNAs (Supplemental Figure 3).

tRNA-half abundance is altered in viral hepatitis associated cancer. In HCC tissue from HBV-infected subjects, RT-qPCR analysis showed that 5′ tRH^{Gly} and 5′ tRH^{Val} abundance was significantly reduced (P<0.005 for both) (Figure 2a). Similar reductions were evident in HCV-associated cancer tissue, but significant only for 5′ tRH^{Val} (P<0.05). We then sequenced small RNAs in cancer tissue from 4 HBV- and 4 HCV-infected subjects. The proportion of reads mapping to tRNA genes was reduced in 4 of 7 samples for which a paired analysis with non-malignant liver was possible, and relatively unchanged in the other 3 (Figure 2b). Although tRNA-derived RNA expression profiles were similar across non-malignant tissues from different subjects, there was substantial variation when compared to cancer tissues (Figure 2c). This suggests that the relative abundance of specific tRNA-derived

RNAs is altered in HCC. Notably, the relative abundance of 5′ tRH^{Gly} was reduced by ~50–60% in both HBV- and HCV-associated cancer (Figure 2d).

tRNA-half abundance correlates with angiogenin levels in HBV-associated cancer. Angiogenin (encoded by the gene ANG) is best known for its role in angiogenesis, but several studies suggest its RNase activity contributes to tRH biogenesis[20,21]. Consistent with this, analysis of previous microarray data obtained from these tissues[14] revealed that ANG mRNA was reduced in both HBV- and HCV-associated cancer compared to non-malignant tissue (P<0.01 and P<0.005, respectively) or uninfected liver (P<0.005 and P=0.01) (Figure 3a). Analysis of data from The Cancer Genome Atlas (https://tcga-data.nci.nih.gov/tcga/) also indicates that ANG expression is reduced in HCC compared to non-malignant tissue, although the difference is significant only for HBV-associated cancer (HBV P<0.005, HCV P=0.12) (Supplemental Figure 5). ANG mRNA abundance correlated strongly with 5′ tRH expression in the HBV-infected subjects we studied (5′ tRH^{Gly}: Spearman's rho=0.67, P<0.01; 5′ tRH^{Val}: rho=0.74, P<0.005) (Figure 3b). Quantitative immunoblot analyses (Supplemental Figure 6) confirmed a correlation between ANG protein abundance and 5′ tRH expression in HBV-associated cancer (5′ tRH^{Gly}: rho=0.83, P<0.005; 5′ tRH^{Val}: rho=0.87, P<0.005) (Figure 3c). ANG was expressed within the cytoplasm of hepatocytes (Figure 3d), and although its expression varied substantially in different tumors (Figure 3e), reductions in ANG expression likely explain the reduced tRH abundance we observed in most HBV-associated cancers. Unfortunately, however, the available tissue sections from these subjects were insufficient to power a formal analysis of the correlation between cytoplasmic versus nuclear expression of ANG and tRH abundance. ANG expression correlated poorly with tRH abundance in HCV-infected livers, suggesting that other factors determine tRH biogenesis.

Discussion

Recent advances in high-throughput sequencing technology have unveiled the complexity and diversity of functional small RNAs. We found that small RNAs derived from tRNAs, specifically 5′ tRNA-halves[9] (5′ tRHs, ~30–35 nts), are abundant in liver, significantly increased during chronic viral infection, and altered in abundance in liver cancer associated with these infections. We do not believe that these tRNA-halves are products of stochastic endonuclease cleavage of tRNAs for several reasons. First, the same tRNA-halves were found to be increased in chronic viral hepatitis across all individuals. Second, each tRNA-half family exhibited a uniform length distribution (e.g., 5′ tRH^{Gly} was represented primarily by reads of length 32–34 in every individual). Third, tRNA-halves were preferentially induced in chronic HBV infection (as compared to chronic HCV infection) in both human and chimpanzee tissue, indicating biological specificity. Finally, tRH abundance was correlated with disease state (cancer versus non-cancer), indicating reproducible sensitivity to the cellular environment.

Several models of disease have been shown to exhibit an increase in tRH abundance, including cultured human airway cells infected with respiratory syncytial virus[22], mice infected with spotted-fever group rickettsia[23], and rats treated with cisplatin[24]. While their function is not well understood, previous work in cell culture suggests that some tRHs promote cell survival, are anti-apoptotic[12], reduce translation[25], and promote the formation of stress granules[26]. Preliminary studies in our laboratory do not support a role for 5′ tRH^{Gly} or 5′ tRH^{Val} in the regulation of global protein translation in human hepatoma cells (Supplemental Figure 7–8); however, more detailed investigation is required to uncover the potential functions of tRHs. It has also been suggested that tRHs may alter the immune response due to their enrichment in mouse lymphoid organs[27], high